JETIR.ORG ISSN: 2349-5162 | ESTD Year : 2014 | Monthly Issue
JOURNAL OF EMERGING TECHNOLOGIES AND INNOVATIVE RESEARCH (JETIR)
An International Scholarly Open Access, Peer-reviewed, Refereed Journal

Flow and Heat Transfer of a Newtonian fluid over a permeable Vertical Stretching Surface Using Optimal Homotopy Analysis Method

Neelufer. Z.Basha

Department of Mathematics, VSK University, Vinayaka Nagar, Ballari-583 105, Karnataka, India

**Corresponding author's E-mail address*:jneelufer198822@gmail.com

Abstract

This paper explores the circulation, as well as heat transfer high qualities in a liquid over a permeable vertical, warmed stretching surface. The nonlinear governing formulas with appropriate border conditions are first cast into dimensionless by utilizing resemblance improvements and afterwards the subsequent conditions are resolved through excellent homotopy examination technique (OHAM). The effects the fluid viscosity, convection specification, speed exponent parameter and also permeability parameter on circulation and also temperature areas are assessed graphically. The assessment reveals a substantial influence of permeability parameter on the flow and warmth transfer high qualities.

Keywords: Mixed convection, permeability, Optimal Homotopy analysis method.

1.Introduction

During the past few years, the study of fluid flow over a stretching sheet has motivated several researchers because of its various industrial and technological applications such as tinning of copper wires, food processing, petroleum drilling, annealing, extraction of polymer sheets, manufacturing of plastic films, crystal growing and paper production etc. Crane [1] reveals that, in a polymer industry, it is not at all possible to avoid considering plastic stretching sheet and hence obtained a similarity solution to the problem of stretching sheet with a linear surface velocity. The transfer of heat around these objects has applications in design of spacecraft, the nuclear reactors and many types of transformers/generators. Further, Carragher and Crane [2] analyzed the heat transfer at a stretching sheet under the condition that the temperature difference between the surface and the free stream, namely, $(T_w - T_\infty)$ is appreciably large (for details see [3-12]).

Most of the problems arising in technological industry are based on mixed convection flow over a heated vertical sheet is of substantial applications and are dare to physicists, engineers and Mathematicians. The findings of such a physical phenomenon will have a definite bearing on plastics, fabrics, and polymer industries. In view of this, Moutsoglou and Chen [13] analyzed numerically the effect of buoyancy parameter on a continuously moving inclined stretching surface. Further, Vajravelu [14] obtained exact solution for hydromagnetic convection at a continuous moving surface with uniform suction and established that when $(T_w > T_\infty)$ the fluid in the boundary-layer will be heated up and thus the free convection currents will set in. Chen [15] extended the model in [14] and analyzed the laminar mixed convection in boundary layers adjacent to a vertical stretching sheet. Recently, Ali et al. [16] examined mixed convection heat transfer in an incompressible viscous fluid over a vertical stretching sheet by taking external magnetic field into account.

It was discovered that the impact of thermal buoyancy is substantial when a home plate is moving vertically up than when it is going on a level aircraft (Kang and Jaluria [17]. Sparrow and Cess [18] and Merkin [19] discussed suction and blowing for an isothermal upright wall surface with cost-free convection. Better, Hooper et al. [20] and Vajravelu [21] inspected the effects of cost-free convection for stream numericallyand also warmth exchange of a viscous liquid practically an infinite, absorptive, upright extending surface. Lately, the influence of radiant heat, Soret as well as Dufour influencesmon mixed convection stream over an upright prolonging sheet was analyzed by Buddy as well as Mondal [22], Samyuktha and also Ravindran [23] Formerly discussed evaluations have actually essentially dealt with the liquid by taking thickness and also thermal conductivity as consistent. It is well known that both viscosity, as well as thermal conductivity differ with temperature level (See Herwing as well as Wickern [24]. For instance, the viscosity of the base liquid, as an example, water lessens certainly by an edge of 240% when a temperature rises from 100 C to 500 C (See Ali [25]. Warmth transfer can be updated by making use of diverse systems and also approaches, for instance, expanding either the warm transfer surface area or the heat transfer coefficient amongst liquid and surface that permits high heat transfer rates in a little quantity. This development is imperative to various contemporary sectors, consisting of generating and also transport. Air conditioning is a standout amongst one of the most important specialized problems facing numerous different ventures, including microelectronics. Furthermore, Prasad et al. [26-31] and Vajravelu et al. [32] have done a wide deal with heat transfer characteristics by taking into consideration Newtonian/non-Newtonian fluid with different geometry. Hence, in this context, today's job is to consider the effects of permeability on the heat transfer move in combined convection regarding the vertically stretching surface area in a Newtonian fluid. The controling nonlinear coupled system of equations for flow as well as heat transfer have actually been lessened to nonlinear coupled differential equations by utilizing an appropriate similarity adjustment as well as are fixed for various evaluations of the physical criteria through Optimal Homotopy Analysis Method (OHAM) [33-34] The obtained outcomes are investigated and also it uncovers that the fluid flow is obviously influenced by the physical criteria. It is expected that the results acquired won't simply offer beneficial data to mechanical applications and additionally supplement the existing literature.

2.Mathematical Analysis

Consider a steady two-dimensional mixed convective boundary layer flow of a liquid over a porous vertical stretching sheet. The origin is located at the slot in the center of the vertical sheet with positive $x-$axis along the sheet and $y-$axis being measured opposite to it as shown in Fig 1.

The flow is restricted in the positive direction of $y-$axis . The flow is caused due to continuous application of two equal and opposite forces along $x-$axis, such that the origin is fixed in the fluid.

The stretching sheet is supposed to have velocity variations and a temperature difference in the following form $U_w = U_0 x^n$ and

$T_w - T_\infty = Ax^r$,

where U_0 a constant is related to the surface stretching speed, x indicates the distance from the slit. n is the velocity exponent parameter, $n > 0 / n < 0$ indicates acceleration/deceleration of the stretching sheet from the slot.

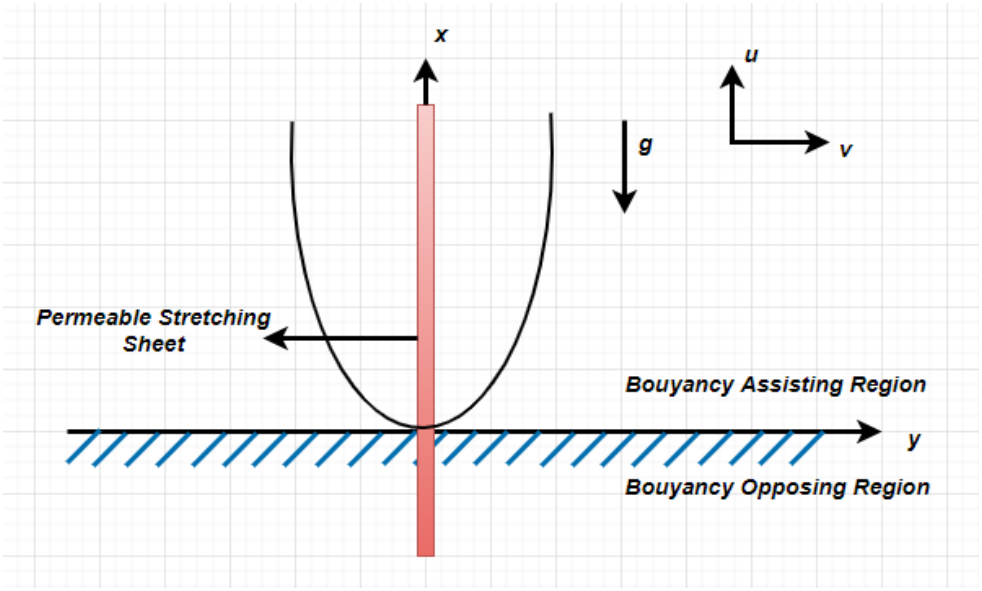

Fig 1: Physical model of the problem

Under these assumptions, with the usual boundary and Boussinesq layer approximation, the continuity, momentum and energy equation are :

$$\frac{\partial u}{\partial x}+\frac{\partial \mathrm{v}}{\partial y}=0 \tag{2}$$

$$u\frac{\partial u}{\partial x}+\mathrm{v}\frac{\partial u}{\partial y}=\nu_\infty\frac{\partial^2 u}{\partial y^2}\pm g\beta_T\left(T-T_\infty\right)-\frac{\nu_\infty}{k}u \tag{3}$$

$$u\frac{\partial T}{\partial x}+\mathrm{v}\frac{\partial T}{\partial y}=\frac{k_\infty}{\rho_\infty C_p}\frac{\partial^2 T}{\partial y^2} \tag{4}$$

where u and v are the fluid velocity components in x and y directions respectively, ρ_∞ is the fluid density, ν_∞ is the kinematic viscosity, g is the acceleration due to gravity, β_T is the thermal expansion coefficient, C_p is the specific heat at constant pressure.

The appropriate boundary conditions on velocity and temperature field are as follows:

$$u=U_w=U_0x^n,\ \mathrm{v}=0,\ T\left(x,y\right)=T_w\left(x\right)=T_\infty+A\,x^r \ \text{ at } \ y=0$$
$$u\to 0,\ T\to T_\infty \ \text{ as } \ y\to\infty \tag{5}$$

Following similarity transformations are invoked in order to convert the system of equations (2) - (4) with boundary conditions (5) into the dimensionless system of ordinary differential equations:

$$\eta=y\sqrt{\frac{U_0(n+1)}{2\nu_\infty}}\,x^{\frac{n-1}{2}} \ \text{ and} \tag{6}$$

$$\psi(x,y)=f(\eta)\sqrt{\frac{2}{n+1}U_0\nu_\infty x^{n+1}} \ \text{ and } \ \theta\left(\eta\right)=\left(T-T_\infty\right)/\left(T_w-T_\infty\right), \tag{7}$$

here ψ is the dimensionless stream function, f and θ are horizontal velocity and temperature of the fluid respectively. As the function $\psi(x,y)$ identically satisfies the continuity Eq (2), Using (7) the velocity components of the fluid in x and y direction can be obtained as

$$u=U_w f'(\eta) \ \text{ and } \ \mathrm{v}=-\sqrt{\nu_\infty\frac{n+1}{2}U_0}\,x^{\frac{n-1}{2}}\left[f(\eta)+\eta f'(\eta)\left(\frac{n-1}{n+1}\right)\right] \tag{8}$$

where the prime denotes differentiation with respect to η. Using similarity transformation momentum and energy equations (3), (4) with the boundary conditions (5) reduces to

$$f'''+ff''-\frac{2n}{n+1}f'^2+\lambda\theta-k_1f'=0, \tag{9}$$

$$\theta''+\mathrm{Pr}\left(f\theta'-\frac{2r}{n+1}f'\theta\right)=0, \tag{10}$$

the dimensionless boundary conditions are

$$f(0)=0,\ f'(0)=1,\ f'(\infty)=0$$
$$\theta(0)=1,\ \theta(\infty)=0. \qquad (11)$$

where $k_1=\frac{\nu_\infty}{Uk}$, $\lambda=\pm\frac{2}{n+1}\frac{Gr_x}{\mathrm{Re}_x^2}$ and $\mathrm{Pr}=\frac{\mu_\infty C_p}{k_\infty}$ are respectively, the permeability parameter, mixed convection or buoyancy parameter and Prandtl number where $Gr_x=\frac{g\beta_T(T_w-T_\infty)x^3}{\nu_\infty^{\,2}}$ is the local Grashof number and $\mathrm{Re}_x=\frac{U_w x}{\nu_\infty}$ is the local Reynolds number. It is clear from the expression that λ is a function of x, to make it self-governing of x, we take $r=2n-1$. Here, $S>0$ corresponds to suction and $S<0$ corresponds to blowing at the permeable sheet. Important physical quantities are Skin friction coefficient C_{fx} and Nusselt number Nu_x which are defined as

$$C_{fx}=\frac{\tau_w}{\rho_\infty U_w^2/2} \text{ and } Nu_x=\frac{xq_w}{k_\infty(T_w-T_\infty)} \qquad (12)$$

where

$$\tau_w=\mu_\infty\left.\frac{\partial u}{\partial y}\right|_{y=0} \text{ and } q_w=-k\left.\frac{\partial T}{\partial y}\right|_{y=0}$$

Using similarity transformations, we get

$$f''(0)=\frac{C_{f_x}(\mathrm{Re}_x)^{1/2}}{2\sqrt{(n+1)/2}} \text{ and}$$

$$-\theta'(0)=Nu_x\frac{(\mathrm{Re}_x)^{-1/2}}{\sqrt{(n+1)/2}}$$

3. Optimal Homotopy Analysis Method:

In order to obtain the analytical solution for the system of highly coupled non- linear equations (9) – (10) with the boundary conditions (11), a highly efficient method, Optimal Homotopy Analysis Method has been employed.

we pick the underlying estimate $f_0(\eta)$, $\theta_0(\eta)$ and linear operators L_f, L_θ for dimensionless velocity and temperature as

$f_0(\eta)=1-e^{-\eta}$ and $\theta_0(\eta)=e^{-\eta}$,

$$L_f=\frac{d^3f}{d\eta^3}-\frac{df}{d\eta} \text{ and } L_\theta=\frac{d^2\theta}{d\eta^2}+\frac{d\theta}{d\eta}$$

The zeroth order deformation equations are given by

$$(1-q)L_1\left[\hat{f}(\eta,q)-f_0(\eta)\right]=q\hbar_f N_1\left[\hat{f}(\eta,q),\hat{\theta}(\eta,q)\right],$$
$$(1-q)L_2\left[\hat{\theta}(\eta,q)-\theta_0(\eta)\right]=q\hbar_\theta N_2\left[\hat{\theta}(\eta,q),\hat{f}(\eta,q)\right],$$

with conditions

$$\hat{f}(0,q)=0,\ \hat{f}'(0,q)=1,\ \hat{f}'(\infty,q)=0,\ \hat{\theta}(0,q)=1,\ \hat{\theta}(\infty,q)=0$$

where $q\in[0,1]$ is an embedding parameter, $\bar{h}\neq 0$ is the convergence control parameter and N_1, N_2 are nonlinear operators defined as

$$N_1=\hat{f}'''(\eta,q)+\hat{f}(\eta,q)\hat{f}''(\eta,q)-\left(\frac{2n}{n+1}\right)\left(\hat{f}'(\eta,q)\right)^2+\lambda\hat{\theta}(\eta,q)-k_1 f',$$

$$N_2=\hat{\theta}''(\eta,q)+\mathrm{Pr}\,\hat{f}(\eta,q)\hat{\theta}'(\eta,q)-\mathrm{Pr}\frac{2r}{n+1}\hat{f}'(\eta,q)\hat{\theta}(\eta,q)$$

we expand $\hat{f}(\eta,q)$ and $\hat{\theta}(\eta,q)$ by means of Taylor's series as

$$\hat{f}(\eta,q) = f_0(\eta) + \sum_{m=1}^{\infty} f_m(\eta) q^m \text{ and } \hat{\theta}(\eta,q) = \theta_0(\eta) + \sum_{m=1}^{\infty} \theta_m(\eta) q^m$$

If the above series converges at $q = 1$, we get the homotopy series solution as

$$f(\eta) = f_0(\eta) + \sum_{m=1}^{\infty} f_m(\eta),\ \theta(\eta) = \theta_0(\eta) + \sum_{m=1}^{\infty} \theta_m(\eta) \text{ and } \varphi(\eta) = \varphi_0(\eta) + \sum_{m=1}^{\infty} \varphi_m(\eta).$$

The optimal value of convergence control parameter $\hbar_f (\neq 0)$ and $\hbar_\theta (\neq 0)$, which helps us to adjust and control the convergence region and the rate of convergence of the homotopy series solution. The average residual error is given by

$$E_m^f = \frac{1}{M+1} \sum_{k=0}^{M} \left(N_f \left(\sum_{n=0}^{m} f_n(\eta_k), \sum_{n=0}^{m} \theta_n(\eta_k) \right)_{\eta_k = k\Delta\eta} \right)^2,$$

$$E_m^\theta = \frac{1}{M+1} \sum_{k=0}^{M} \left(N_\theta \left(\sum_{n=0}^{m} f_n(\eta_k), \sum_{n=0}^{m} \theta_n(\eta_k) \right)_{\eta_k = k\Delta\eta} \right)^2$$

and $E_m{}^t = E_m{}^f + E_m{}^\theta$

(For details see Liao (32)). where $E_m{}^t$ stands for a total squared residual error and $\eta_k = k\Delta\eta = \frac{k}{M}, k = 0,1,2,....M$. Now we minimize the error function $E_m{}^f$ and $E_m{}^\theta$ in $\hbar_f$ and $\hbar_\theta$ and obtain the optimal value of $\hbar_f$ and $\hbar_\theta$. Substituting these optimal values of $\hbar_f$ and $\hbar_\theta$ in in the series solution, we get the approximate solutions of equations (9) and (10) which satisfies the conditions (11). For the assurance of the validity of this method

- Residual error graphs are plotted for the assurance of accuracy and efficiency of OHAM.
- $-f''(0)$ and $\theta'(0)$ obtained via OHAM has been compared with Vajravelu et al. [32] for some special cases and the results are found to be in excellent agreement as shown in Table 1.

4. Results and discussion

The system of equations (9) and (10) with boundary conditions (11) is solved using semi-analytical method, OHAM. Effects various parameters are displayed graphically in Figures 2–8. These figures represent variations in horizontal velocity profile $f'(\eta)$ and temperature profile $\theta(\eta)$ for different values of the pertinent parameters. The computed values of skin friction $f''(0)$ and wall temperature gradient $\theta'(0)$ are tabulated in Table 2.

Fig. 2 illustrate the effects of growing values of n and k_1 on $f'(\eta)$ and $\theta(\eta)$ respectively. Fig. 2(a) depicts that, with an increase of n and k_1, velocity decreases and opposes the horizontal flow for fixed η. In the case of $\theta(\eta)$; the growing values of n increases the temperature profile whereas the opposite effect is observed in case of k_1. The impact of λ on $f'(\eta)$ and $\theta(\eta)$ is represented in Fig. 3(a-b). The finite value of λ $(\lambda \neq 0)$ uncovers the thermal buoyancy effect which tends to upgrade the flow along the surface. Increment in λ leads to an enhancement in $f'(\eta)$. Physically, $\lambda > 0$ means heating of the fluid or cooling of the surface, $\lambda < 0$ means cooling of the fluid or heating of the surface and $\lambda = 0$ indicates the absence of the mixed convection parameter. Increase in λ means an increase in the temperature difference $(\Delta T = T_w - T_\infty)$ and enhanced convection which leads to an enhancement in $f'(\eta)$, and thus an increase in the momentum boundary layer thickness is observed. The effect of λ on temperature profile is quite opposite, that is, the temperature field is suppressed and consequently thermal boundary layer thickness becomes thinner. Hence the magnitude of the rate of heat transfer from the surface increases (See fig 3(b) and Table 2). Fig. 4 exhibits the effect of Pr going from 1 to 10 for different estimations of *n*. Increment in Pr brings about a lessening of thermal boundary layer thickness and is due to k_∞. Subsequently, the improvement in the cooling of the heated surface can be done by choosing a proper coolant with a large Pr and increase in *n* gives a similar effect.

Finally, Fig. 5(a-c) shows the streamline patterns for different values of λ. The residual errors for $f'(\eta)$ and $\theta(\eta)$ are presented in Fig. 6(a– b), which show evidence of meticulousness and convergence of the OHAM.

5.Conclusion

Some of the interesting results are as follows:

- For growing values of velocity exponent parameter and permeability parameter, there is decrease in the horizontal velocity profile and consequently the momentum boundary layer thickness decreases.
- As the velocity exponent parameter enhances, there is enhancement in the temperature profile and as a result of it, the thermal boundary layer thickness increases.
- The impact of increasing values of mixed convection parameter is to increase the velocity profile and the reverse effect is observed in case of temperature profile.
- The increasing values of Prandtl number, lessen the momentum boundary later thickness and the reverse effect is observed in case of temperature profile.

References

[1] Crane, L.J., Flow past a stretching plate, ZAMP. 21, 645–655, (1970).

[2] Carragher, P., and Carane, L.J., Heat transfer on a continuous stretching sheet, Z. Angew. Math. Mech. 62, 564–565, (1982).

[3] Grubka, L.J., and Bobba, K.M., Heat transfer characteristics of a continuous stretching surface with variable temperature, J. Heat and Mass Transfer. 107, 248–250, (1985).

[4] Chen, C.K., and Char, M.I., Heat transfer of a continuous stretching surface with suction or blowing, J. Math. Anal Appl. 135, 568–580, (1988).

[5] Ali, M. E., Heat transfer characteristics of a continuous stretching surface, Heat Mass Transfer. 29, 227-234, (1994).

[6] Vajravelu, K., Viscous flow over a nonlinearly stretching sheet, Applied Mathematics and Computation. 124, 281–288, (2001).

[7] Ishak, A., Nazar, R.., and Pop, I., Hydromagnetic flow and heat transfer adjacent to a stretching vertical sheet, Heat Mass Transfer. 44, 921– 927, (2008).

[8] Cortell, R., Viscous flow and heat transfer over a nonlinearly stretching sheet, Applied Mathematics and Computation. 184, 864–873, (2007).

[9] Bikash Sahoo., Flow and heat transfer of a non-Newtonian fluid past a stretching sheet with partial slip, Communications in Nonlinear Science and Numerical Simulation. 15, 602–615, (2010).

[10] Javed, T., Abbas, Z., Sajid, M., and Ali, N., Heat transfer analysis for a hydromagnetic viscous fluid over a non-linear shrinking sheet, International Journal of Heat and Mass Transfer. 54, 2034–2042, (2011).

[11] Fazle Mabood, Khan, W.A., and Ismail, W.A., MHD flow over exponential radiating stretching sheet using homotopy analysis method, doi:10.1016/j.jksues.2014.06.001.

[12] Hossam S. Hassan., Symmetry Analysis for MHD Viscous Flow and Heat Transfer over a Stretching Sheet, Applied Mathematics. 6, 78-94, (2015).

[13] Moutsoglou, A., and Chen, T. S., Buoyancy effects in boundary layers on inclined, continuous moving sheets, ASME Journal of Heat Transfer. 102, 371-373, (1980).

[14] Vajravelu, K., Convection heat transfer at a stretching sheet with suction or blowing, J. Math. Anal. Appl. 188, 1002–1011, (1994).

[15] Chen, C.H., Laminar mixed convection adjacent to vertical continuously stretching sheets, Heat Mass Transfer. 33, 471-476, (1998).

[16] Ali, F. M., Nazar, R., Arifini, N. M., and Pop, I., Mixed convection stagnation-point flow on vertical stretching sheet with external magnetic field, Appl. Math. Mech. -Engl. Ed., 35, 155–166, (2014).

[17] B. H. Kang and Y. Jaluria, Thermal modeling of the continuous casting process, J Thermophysics and Heat transfer **1,** 139-147, (1993).

[18] E. M. Sparrow, R. D. Cess, Free convection with blowing or suction, J. Heat Tran. 83, 387–396, (1961).

[19] J. H. Merkin, Free convection with blowing and suction, Int. J. Heat Mass Tran. 15 (1972) 989–999.

[20] W.B. Hooper, T.S. Chen and B.F. Armaly, Mixed convection from a vertical plate in porous media with surface injection or suction, Numerical Heat Transfer, Part A: Applications 25 (1994) 317–329.
[21] K. Vajravelu, Convection heat transfer at a stretching sheet with suction or blowing, J Math Anal Appl. 188 (1994) 1002–11.
[22] D. Pal, H. Mondal, Influence of chemical reaction and thermal radiation on mixed convection heat and mass transfer over a stretching sheet in Darcian porous medium with Soret and Dufour effects, Energy. Convers. Manage. 62 (2012) 102–108.
[23] N. Samyuktha, R. Ravindran, Thermal Radiation Effect on Mixed Convection Flow over a Vertical Stretching Sheet Embedded in a Porous Medium with Suction (Injection), International Conference on Computational Heat and Mass Transfer, 2015
[24] H. Herwig and G Wickern, The effect of variable properties on laminar boundary layer flow, Wärme- und Stoffibertragung 20 (1986) 47-57.
[25] M. E. Ali, The effect of variable viscosity on mixed convective heat transfer along a vertical moving surface, International Journal of Thermal Sciences 45 (2006).
[26] H.Vaidya, C. Rajashekhar, G. Manjunatha, K.V. Prasad, Effect of variable liquid properties on peristaltic flow of a Rabinowitsch fluid in an inclined convective porous channel, The European Physical Journal Plus, Vol.134(5), pp.1-14, 2019.
[27] H. Vaidya, C. Rajashekhar, G. Manjunatha, K.V. Prasad, Rheological Properties and Peristalsis of Rabinowitsch Fluid Through Compliant Porous Walls in an Inclined Channel, Journal of Nanofluids, Vol. 8(5), pp.970-979, 2019.
[28] H. Vaidya, M. Gudekote, R. Choudhari, K. V. Prasad, Role of slip and heat transfer on peristaltic transport of Herschel-Bulkley fluid through an elastic tube, Multidiscipline Modeling in Materials and Structures, Vol. 14(5), 2018.
[29] K.V. Prasad, K. Vajravelu, H. Vaidya, Hall effect on MHD flow and heat transfer over a stretching sheet with variable thickness, International Journal for Computational Methods in Engineering Science and Mechanics, Vol. 17(4), pp.288-297, 2016.
[30] G. Manjunatha, C. Rajashekhar, H. Vaidya, K.V. Prasad, O.D. Makinde, J.U. Viharika, Impact of variable transport properties and slip effects on MHD Jeffrey fluid flow through channel, Arabian Journal for Science and Engineering, Vol. 45(1), pp.417-428,2020.
[31] H. Vaidya, C. Rajashekhar, B.B. Divya, G Manjunatha, K.V. Prasad, IL Animasaun, Influence of transport properties on the peristaltic MHD Jeffrey fluid flow through a porous asymmetric tapered channel, Results in Physics, Vol.18, pp. 103295, 2020
[32] K. Vajravelu, K. V. Prasad and Chiu-on Ng, Unsteady convective boundary layer flow of a viscous fluid at a vertical surface with variable fluid properties, Nonlinear analysis, Real world applications 14 (2013) 455-464.
[33] S. Liao, Beyond perturbation: Introduction to homotopy analysis method, Chapman & Hall/CRC Press, London, 2003.
[34] T. Fan and X. You, Optimal homotopy analysis method for nonlinear differential equations in the boundary layer, Numer. Algor. 62 (2013) 337-354.

Table 1: Comparison of $-f''(0)$ and $\theta'(0)$ for different values of λ when $\Pr = 1,\ n = 5.$

λ	$-f''(0)$				$\theta'(0)$			
	Vajravelu et al. [32]	Present Result			Vajravelu et al. [32]	Present Result		
		OHAM	$-\hbar_f$	E_8^f		OHAM	$-\hbar_f$	E_8^f
-0.5	0.946425	0.946422	1.365484	3.5×10^{-9}	-1.53881	-1.53885	1.321631	7.8×10^{-9}
0.0	0.844632	0.844645	1.382598	2.5×10^{-8}	-1.56073	-1.56074	1.354896	2.5×10^{-8}
0.5	0.747777	0.747789	1.984531	1.4×10^{-7}	-1.5799	-1.57992	1.662654	1.3×10^{-7}
1.0	0.654721	0.654701	1.516548	6.5×10^{-6}	-1.59699	-1.59694	1.626530	2.6×10^{-7}

Table 2: Values of $f''(0)$ and $\theta'(0)$ with required CPU time (in seconds) for different values of the physical parameters.

Pr	λ	k_1	$n=1$			$n=2$			$n=5$		
			$f''(0)$	$\theta'(0)$	CPU Time	$f''(0)$	$\theta'(0)$	CPU Time	$f''(0)$	$\theta'(0)$	CPU Time
2.0	0.5	**0.1**	-0.653467	-1.505170	2870	-0.746064	-1.937660	1933	-0.827716	-2.297050	2134
		0.2	-0.692731	-1.515200	1486	-0.792385	-1.938200	1917	-0.880263	-2.308570	2104
		0.3	-0.741893	-1.526482	1924	-0.850670	-1.940700	1893	-0.946405	-2.327780	2049
		0.4	-0.798778	-1.545689	1903	-0.918464	-1.959490	1865	-1.023420	-2.365060	2004
		0.5	-0.944808	-1.558976	6222	-1.094410	-1.969410	1859	-1.224340	-2.370770	6862
2.0	**-0.5**	0.1	-0.921286	-1.460100	1892	-0.987288	-1.895900	2050	-1.052660	-2.257640	2111
	0.0		-0.804801	-1.480440	1609	-0.888405	-1.913670	2131	-0.965351	-2.273580	1883
	0.5		-0.692731	-1.498720	1872	-0.792385	-1.930200	2008	-0.880263	-2.288570	2141
	1.0		-0.584083	-1.515370	1891	-0.698817	-1.945660	2006	-0.796790	-2.302800	1977
1.0	0.5	0.5	-0.648442	-1.018850	729	-0.752532	-1.316820	949	-0.843345	-1.565230	1225
2.0			-0.692731	-1.498720	1859	-0.792385	-1.930200	1871	-0.880263	-2.288570	2258
5.0			-0.739404	-2.456710	8700	-0.834646	-3.154650	1393	-0.919576	-3.732050	10101
7.0			-0.75325	-2.931690	6181	-0.847187	-3.759270	6884	-0.931527	-4.449920	7736
10.0			-0.765932	-3.541930	3741	-0.858237	-4.578950	3723	-0.942239	-5.390300	6636

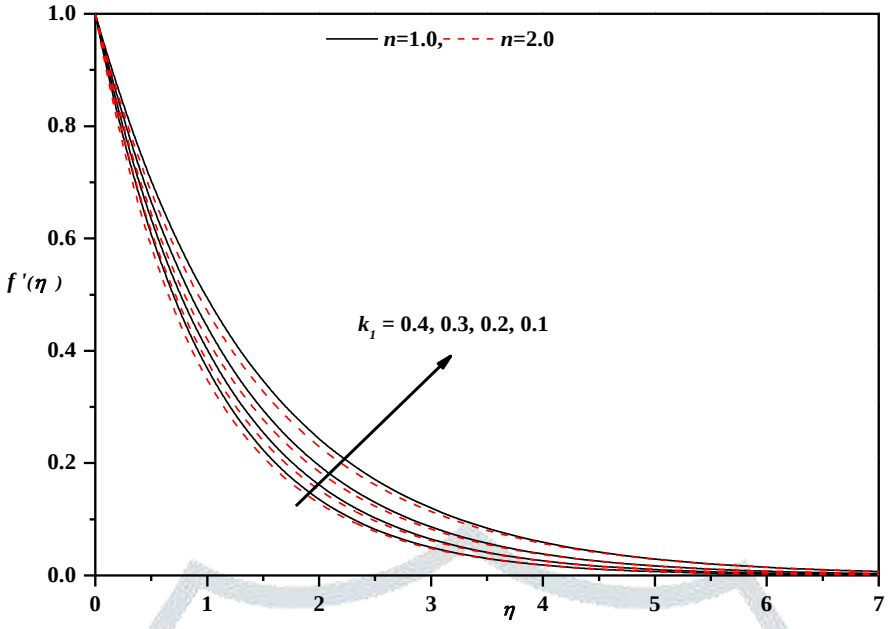

Fig 2(a):Horizontal velocity profile for different values of k_1 and n with Pr = 1.0, Nt =0.1, Nb=0.1, Le =0.22

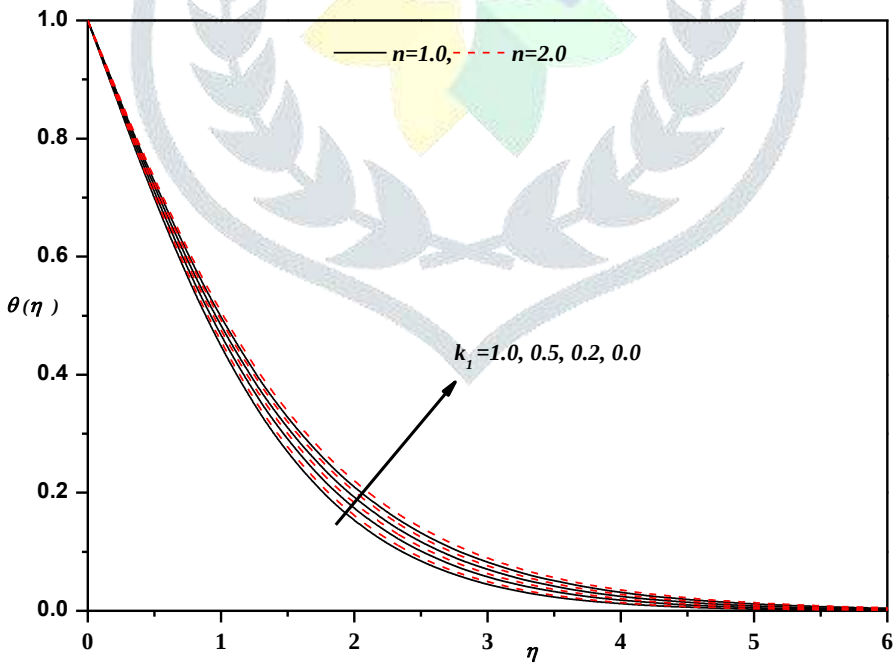

Fig 2(b): Temperature profile for different values of k1 and n with Pr =1.0, Nt =0.1, Nb =0.1, Le =0.22

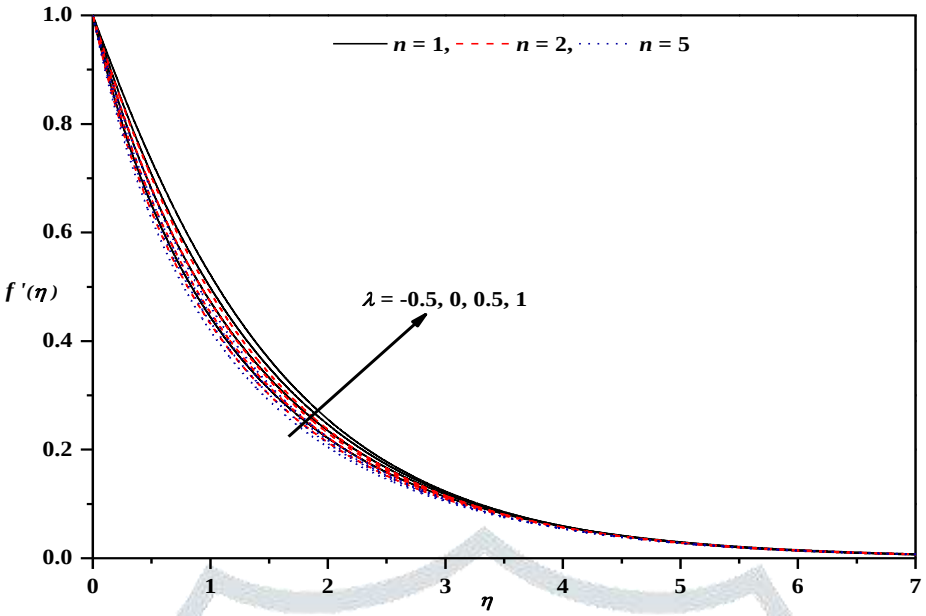

Fig 3(a) : Horizontal velocity profile for different values of λ and n with Pr = 2.

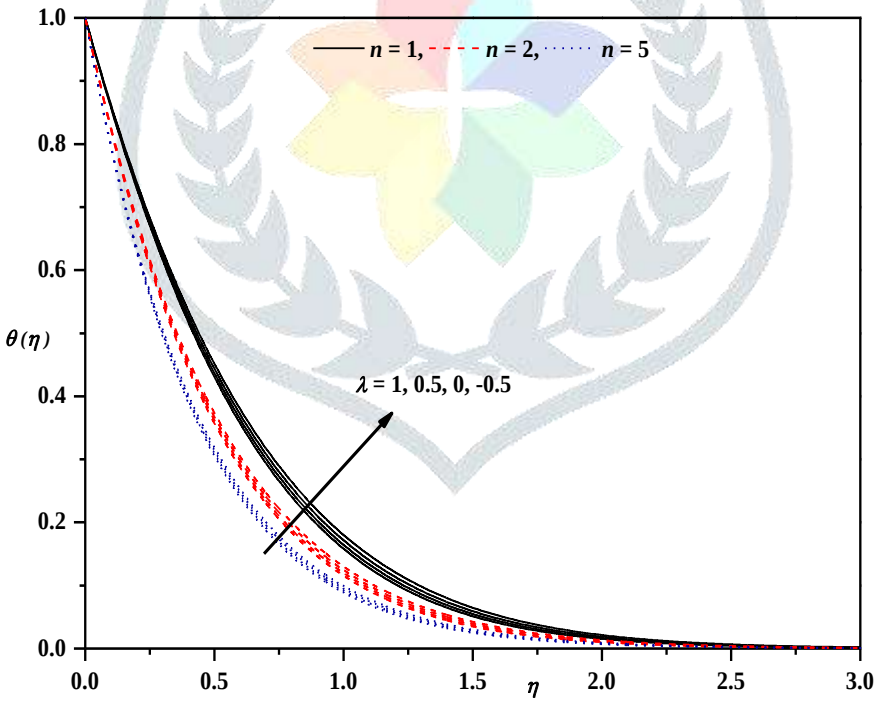

Fig 3(b) : Temperature profile for different values of λ and n with Pr = 2.

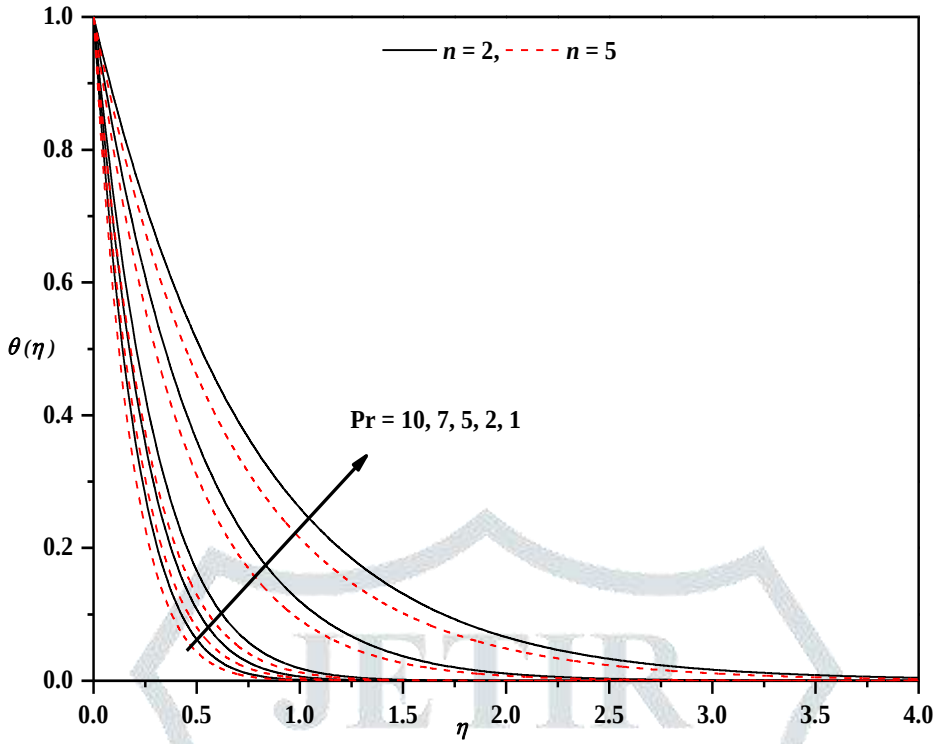

Fig 4 : Temperature profile for different values of Pr and *n* with $\lambda = 0.5$.

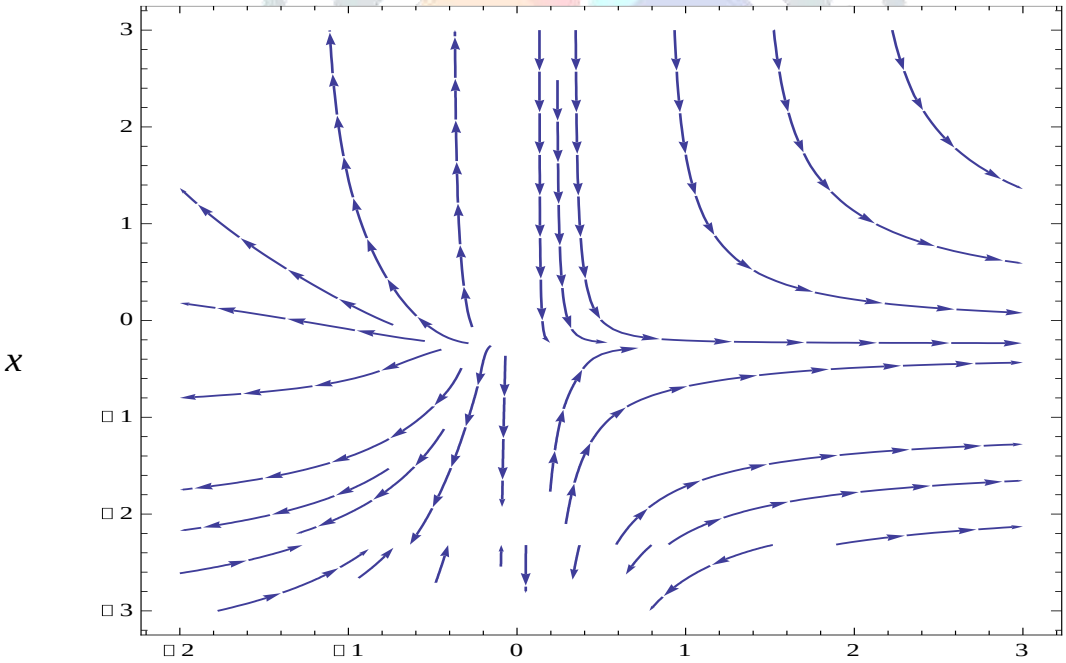

Fig 5(a): Streamline pattern plot when k_1=0.1, $\Pr = 2, n = 2, \lambda = 0.5$.

η

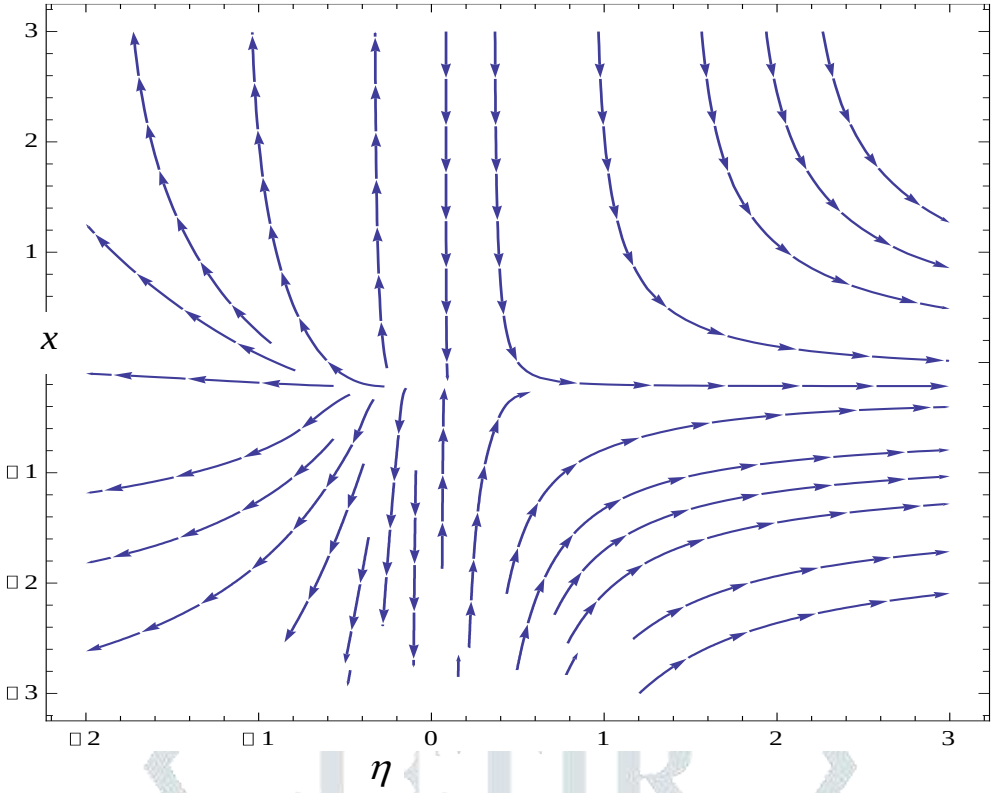

Fig 5(b): Streamline pattern plot when $\Pr = 2, n = 2, \lambda = 0.5.$

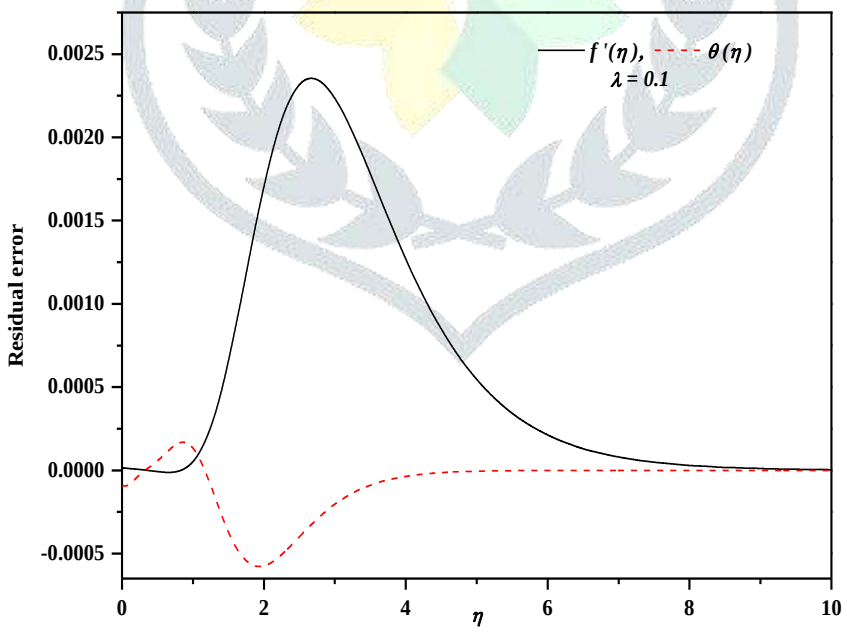

Fig 6(a) : Residual error profile forHorizontal velocity and temperature for k_1=0.1, Pr = 2, λ = 0.5, n = 2.

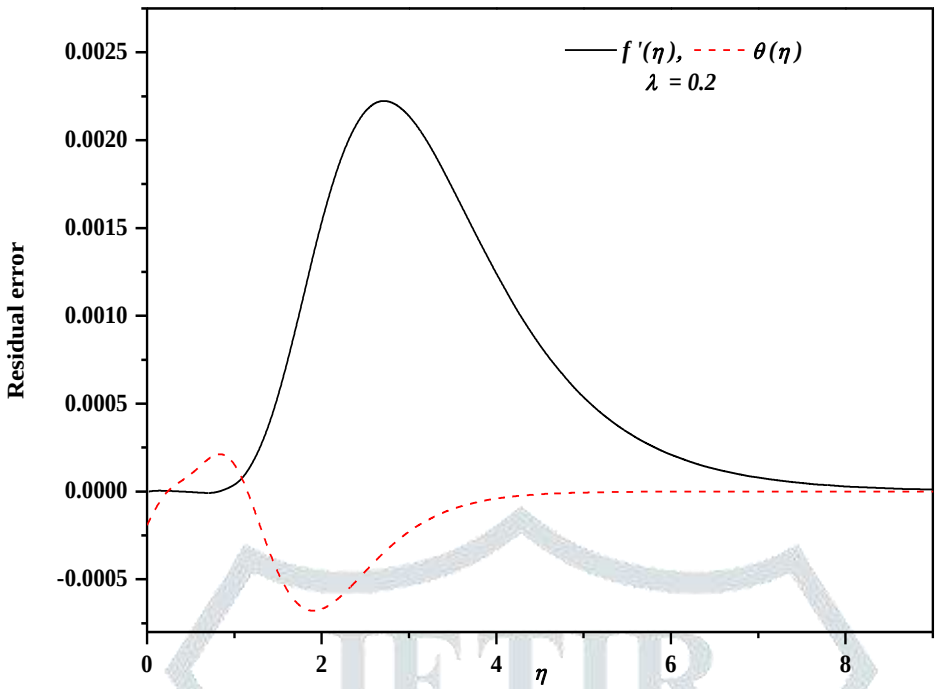

Fig 6(b) : Residual error profile forHorizontal velocity and temperature for k_1=0.1, Pr = 2, λ = 0.5, n = 2.